ELSEVIER

Journal of Nuclear Materials 249 (1997) 33–38

journal of nuclear materials

Investigations on the transformation behavior of the intermetallic phase $(Fe, Cr)_2Al_5$ formed on MANET II steel by aluminizing

K. Stein-Fechner, J. Konys *, O. Wedemeyer

Forschungszentrum Karlsruhe GmbH, Institut für Materialforschung III, Postfach 3640, D-76021 Karlsruhe, Germany

Received 25 February 1997; accepted 14 June 1997

Abstract

The present work describes investigations on the transformation behavior of the intermetallic phase $(Fe, Cr)_2Al_5$ which forms on martensitic 10%Cr steel during aluminizing. In order to improve the mechanical properties of the coating and to incorporate the metallic Al overlayer, a subsequent heat treatment is necessary after aluminizing. Heat treatments were carried out in Ar at 700°C and 1075°C for several exposure times. It was found at 700°C that the $(Fe, Cr)_2Al_5$ scale starts to transform into the softer (Fe, Cr)Al phase (referring to hardness) at the scale-substrate interface. This process is time dependent. The (Fe, Cr)Al phase gets further transformed into the α-Fe(Cr, Al) solid solution. After heat treatment at 1075°C for 0.5 h the $(Fe, Cr)_2Al_5$ scale is completely transformed. The resulting scale can be subdivided into an upper layer of (Fe, Cr)Al phase, an intermediate band of pores and a lower layer of α-Fe(Al, Cr) solid solution. © 1997 Elsevier Science B.V.

1. Introduction

In the fusion technology there is need for tritium permeation barriers on low activation steels [1–3]. It is known that thin alumina scales can reduce the T-permeation rate by several orders of magnitude [4]. However, ceramic scales tend to fail already at very low deformations. Cracks within the alumina scale would indicate preferential paths for the T-permeation through the steel substrate. A suitable coating for technical application must therefore have the potential for rehealing of cracks. It seems that a coating of the (Fe, Cr)Al phase or α-Fe(Cr, Al) solid solution should be able to fulfil this demand and also shows acceptable mechanical properties. Several methods have been developed to produce such scale systems on martensitic 8–10%Cr steels [5–9]. By hot dip aluminizing for example, firstly a hard and brittle intermetallic $(Fe, Cr)_2Al_5$ scale is formed. A subsequent heat treatment transforms this scale into desired softer phases [10]. This paper describes the transformation behavior of the intermetallic $(Fe, Cr)_2Al_5$ scale at 700°C and 1075°C. These temperatures were chosen for the investigation since they play an important role in view of the mechanical properties of the martensitic steel substrate. Former investigations have shown that the hot dip aluminizing process at 750°C has no effect on the martensitic structure of MANET steel due to the rapidity of this process at temperatures below the A_{c1b} temperature (A_{c1b}: α–γ transformation start) of the MANET steel (A_{c1b} of the MANET = 780°C). The question which arises now is whether or not a heat treatment of the intermetallic scale below the A_{c1b} temperature for short times is sufficient for a complete phase transformation. If temperatures higher than A_{c1b} are necessary for the phase transformation or the complete phase transformation at 700°C would take too long time and therefore soften the martensitic structure, the substrate-coating system has to undergo a complete reaustenititing and tempering process to reproduce the mechanical properties of the steel substrate, i.e., the system has to see 1075°C for 0.5 h and subsequently 750°C for 2 h.

---

* Corresponding author. Tel.: +49-7247 823 720; fax: +49-7247 823 956; e-mail: juergen.konys@imf.fzk.de.

PII S0022-3115(97)00208-0

2. Materials and experimental procedure

The chemical analysis of the aluminized MANET-steel is given in Table 1. The material had been received as a 4 mm thick sheet in tempered condition (NET-heat No. 50806 produced by Saarstahl Völklingen, Germany). Sample sheets (50 mm × 15 mm × 1.5 mm) have been machined, each having a small hole on one side for fixing during the aluminizing process. The specimens were sandblasted, degreased in acetone and finally cleaned ultrasonically in ethanol. In order to improve the wettability of the steel surfaces with the Al melt the specimens were dipped into a saturated solution of KCl, NaCl and Na_3AlF_6 (ratio 5:4:1) in water and dried prior to aluminizing. For the immersion process an Al melt of 99.5% purity has been used with main impurities being Fe and Si.

Aluminizing has been carried out by using the facility described in Ref. [11]. On its bottom a glove box is connected gas tight to a heated alumina crucible. The atmosphere is a reducing Ar–5%H_2 mixture to prevent oxidation of the Al melt. The alumina crucible was filled with small Al pieces and heated up to 700°C. The temperature was measured by a NiCr–Ni thermocouple which was protected by an alumina tube and placed directly in the Al melt. The sample sheets, fixed by a hook and stainless steel wire to a crane system, were dipped into the Al melt. After 10 s of exposure the samples were pulled out. Cooling down took place in the glove box by natural cooling. Two samples were dipped into a 750°C hot Al melt for 20 s.

In order to investigate the transformation behavior of the brittle intermetallic $(Fe, Cr)_2Al_5$ phase which forms during the aluminizing process several heat treatments were carried out. The aluminized samples were cut into small pieces of about 10 mm × 15 mm × 1.5 mm, cleaned ultrasonically in ethanol, dried and placed in alumina crucibles. Only those parts of the aluminized specimens were used which showed a uniform Al overlayer. For the heat treatment the alumina crucibles were positioned in a horizontal quartz pipe within the hot zone of a furnace. The working rig was flushed with Ar 6.0, and finally a flow rate of 5 l/h and a pressure of 1.25 bar were adjusted. The heating rate was about 25 K/min. The time and temperature schedules of the heat treatment are listed in Table 2. Sample cooling after the heat treatment was by furnace cooling.

Metallographic cross-sections were prepared to study the coating after aluminizing and subsequent heat treatment, respectively. Analytical investigations were carried out using optical microscopy, SEM/EDX and EPMA. The hardness was measured by Vickers hardness testing (HV 0.05).

Table 1
Chemical composition of MANET II (wt%)

C	Si	Mn	P	S	Cr	Ni	Mo	V	Nb	Fe
0.10	0.18	0.76	0.004	0.005	10.37	0.65	0.58	0.21	0.16	Bal.

Table 2
Conditions of the heat treatment after the aluminizing process

Specimen number	Aluminizing conditions	Heat treatment after aluminizing
1	700°C/10 s	1075°C/0.5 h
2	700°C/10 s	700°C/100 h
3	700°C/10 s	700°C/30 h
4	750°C/20 s	700°C/72 h
5	750°C/20 s	700°C/2 h

3. Results

3.1. Aluminized samples

After hot dip aluminizing the sample sheets were homogeneously covered by an overlayer of solidified Al melt. Only on the bottom side of the samples and around the fixing hole an Al drop had solidified during the cooling phase since no tools were used to remove the excess melt. Tiny unwetted spots could be observed sometimes on samples which were immersed for 10 s at 700°C.

Cross-section examinations have shown that the Al overlayer had a thickness of about 15–25 μm. The structure of the formed intermetallic scale beneath the overlayer was identical for both aluminizing conditions whereas the thickness of the intermetallic scale itself varied. The maximum scale thickness, not including the solidified Al on top, was measured at 10 different positions, and the average value was calculated. The scale thickness was determined to be 18 μm and 41 μm for the 700°C/10 s and 750°C/20 s samples, respectively. As an example the cross-sectional view of an aluminized sample (750°C/20 s) is shown in Fig. 1. The interface between the substrate

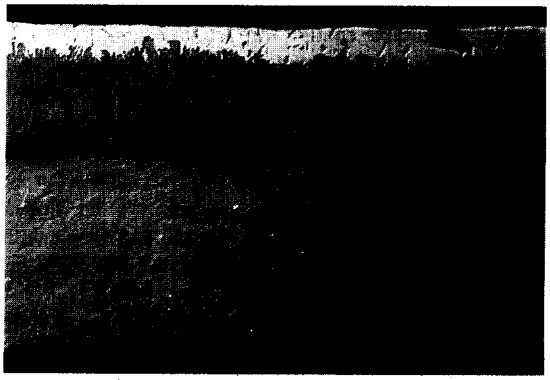

Fig. 1. Cross-section of an aluminized sample (750°C/20 s).

and the intermetallic scale is smooth although the scale grew somewhat tongue-like into the substrate. The interface between the Al overlayer and the intermetallic scale appears very inhomogeneous. This pattern is a good indication for two competitive processes: crystal growth and desolution of the formed crystals and transport into the Al melt. Across the whole scale sharp cracks can be observed.

SEM/EDX point analyses have shown that the main part of the scale has a composition of 70–72 at.% Al, 26–28 at.% Fe and about 2 at.% Cr. Comparing these results with the binary Fe–Al phase diagram [12] and X-ray diffraction measurements [13] it is obvious, that the formed scale corresponds to the binary $(Fe, Cr)_2Al_5$ phase. The formation of a ternary Fe–Al–Cr phase was not detected. Although the Al-rich corner of the Fe–Al–Cr phase diagram [14] is not fully investigated, the measured diffraction data are fitting perfectly to the binary Fe_2Al_5 phase. This indicates, that there must be a solubility in the range of a few percent for Cr in the Fe_2Al_5 phase. Just beneath the metallic Al overlayer an Al concentration was measured which is evidence for the existence of the $(Fe, Cr)Al_3$ phase (it has been assumed that there is a slight solubility for Cr in the binary $FeAl_3$ phase, too). Also, the precipitates in the Al melt were found to be $(Fe, Cr)Al_3$ phase. The hardness of the formed intermetallic scale was about 1000–1100 HV0.05.

3.2. Aluminized and subsequent heat treated samples

3.2.1. Heat treatment at 700°C

Several heat treatments were carried out at 700°C with varying exposure times in order to investigate the transformation behavior of the intermetallic scale. In Fig. 2a and b cross-sectional views of two heat treated samples are presented for exposure times of 30 h and 72 h, respectively. It was found after heat treatment at 700°C that the Al overlayer was completely incorporated into the steel substrate by diffusion. Cross-sectional examinations have shown that the surface of the samples is extremely inhomogeneous. Near the surface many pores have formed in the intermetallic scale. Also, some cracks could be observed which grew from the sample surface through the intermetallic scale. Sometimes spallation of the perforated upper layer of the scale was observed. In Fig. 2a an about 9 μm thick grey band can be observed beneath the intermetallic scale. The interface to the intermetallic scale above forms a sharp boundary. The thickness of the grey band has increased to 14 μm after longer exposure times, Fig. 2b. Some pores have formed between the grey band and the substrate after 72 h. Also, needle like precipitations could be observed in the substrate beneath the grey band.

EPMA results of the samples shown in Fig. 2a and b are presented in Fig. 3a and b, respectively. The intermetallic scale beneath the sample surface mainly consists of about 70–72 at.% Al, 26–28 at.% Fe and about 2 at.% Cr and corresponds to the $(Fe, Cr)_2Al_5$ phase. As to be seen in Fig. 3a the $(Fe, Cr)_2Al_5$ scale started to transform at the scale-steel interface. The transformed zone is in total about 20 μm thick after 30 h heat treatment. A small plateau is indicated at about 48 at.% Al before the concentration of Al decreases further. Corresponding to the binary Fe–Al phase diagram [12] (which is used here instead of the ternary Fe–Cr–Al phase diagram), the FeAl phase exists for Al-concentrations between 24 and 50 at.% Al at 700°C. The concentration profile in Fig. 3a shows that the zone between 24 and 50 at.% Al is about 10 μm thick. This value corresponds well to the thickness of the grey band beneath the intermetallic scale in Fig. 2a. The concentration profile in Fig. 3b shows that the total thickness of the transformed zone has increased to about 35 μm after 72 h heat treatment. The zone between 24 and 50 at.% Al, i.e., the area where the (Fe, Cr)Al phase exists, is about 16 μm thick after 72 h exposure. This value corresponds well to the thickness of the grey band in Fig. 2b. According to

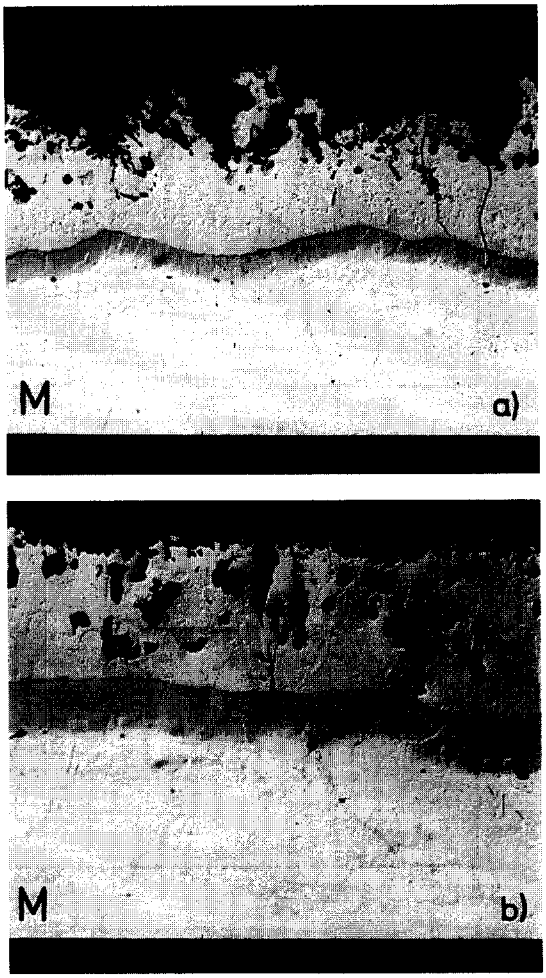

Fig. 2. Cross-section of aluminized MANET samples, heat treated at 700°C, (a) 30 h, (b) 72 h.

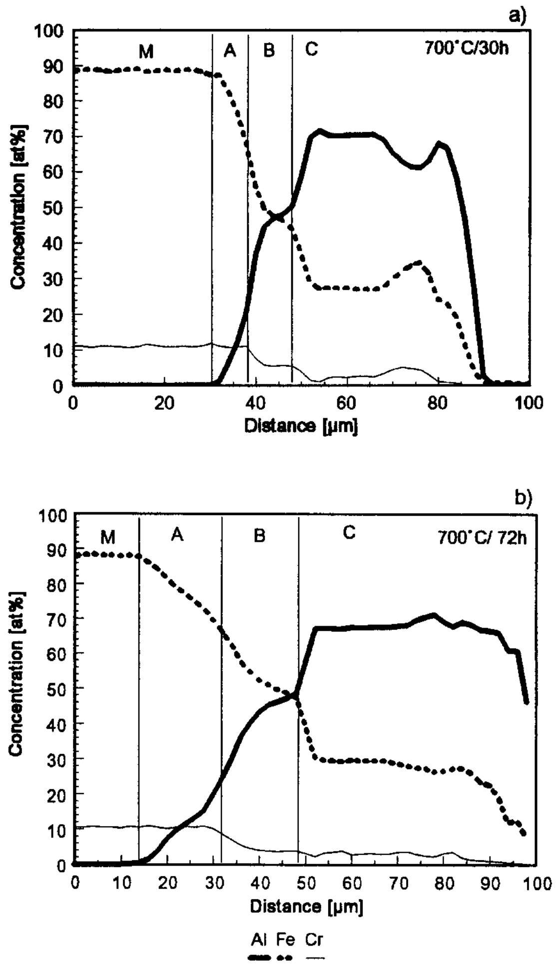

Fig. 3. EPMA line scans of aluminized MANET samples, heat treated at 700°C, (a) 30 h, (b) 72 h. A: α-Fe(Cr, Al); B: (Fe, Cr)Al; C: (Fe, Cr)$_2$Al$_5$; M: matrix.

the binary Fe–Al phase diagram solely the α-Fe(Al) solid solution exists for Al concentrations between 0–24 at.% Al at 700°C. This zone is however not clearly visible in Fig. 2a and b, respectively.

In order to determine the growth rate law of the transformed scale, including the (Fe, Cr)Al phase and the α-Fe(Cr, Al) solid solution, in Fig. 4 the thickness of the transformed scale versus the exposure time is shown in a double logarithmic scale. Assuming the rate follows the function

$$S^n = kt, \quad (1)$$

where S is the thickness of the transformed scale, k is the reaction constant, t is the exposure time and n is the exponent, the thickness should be a linear function of exposure time in a double logarithmic graph. The value of n was calculated by regression to be 2.6, i.e., a slightly superparabolic growth rate is valid.

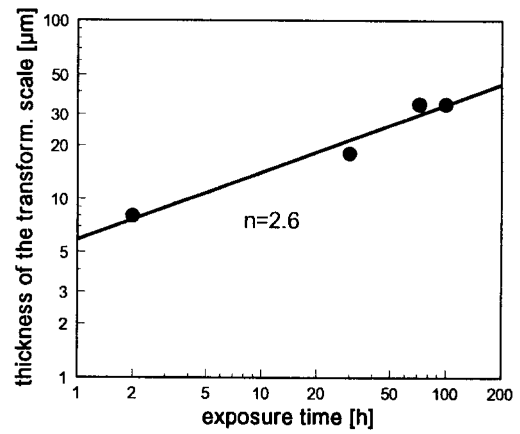

Fig. 4. Total thickness of the transformed scale versus exposure time at 700°C. n is the exponent of the equation $S^n = kt$ which describes the growth rate of the transformed scale.

The hardness of the remaining intermetallic scale was about 1050 HV0.05. The hardness of the formed (Fe, Cr)Al phase was much lower and varied between 420 and 480 HV0.05. Due to the small thickness of the α-Fe(Cr, Al) solid solution zone beneath the (Fe, Cr)Al layer it was not possible to determine a reliable hardness value.

3.2.2. Heat treatment at 1075°C

The scale structure existing after the heat treatment at 1075°C for 0.5 h is shown in Fig. 5. The scale which has a total thickness of about 250 µm can be subdivided into an upper layer of about 100 µm, an about 25 µm thick intermediate band of high porosity and a lower layer of about 125 µm thickness. The interface to the substrate beneath is indicated as a sharp boundary. The sample surface is rather inhomogeneous. In the upper layer of the scale, near to the surface, some pores have formed up to 35 µm in size but no cracks could be observed across the

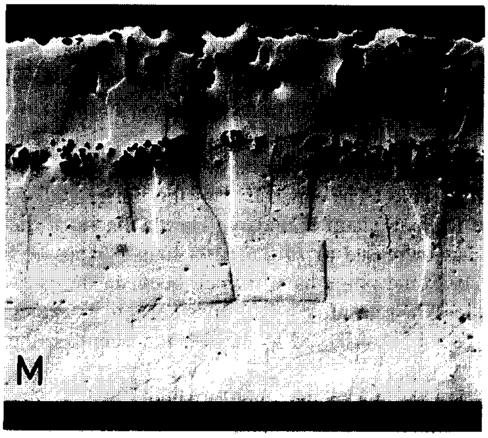

Fig. 5. Cross-section of aluminized MANET sample, heat treated at 1075°C for 0.5 h.

scale. The pores of the intermediate part of the scale are much smaller compared to the pores beneath the sample surface and about 3–5 μm in size. The pore density however is clearly higher in the intermediate part. The structure of the scale is characterized by large grains of up to 100 μm in width oriented perpendicular to the surface. In the lower layer of the scale fine precipitations can be observed which are homogeneously distributed. The grain structure beneath the scale has the typical appearance of a martensitic substrate.

EPMA results are shown in Fig. 6. It can be seen that the intermetallic (Fe, Cr)$_2$Al$_5$ phase has completely transformed after the heat treatment at 1075°C. There is solely Al on the surface indicating the existence of an alumina rich layer on top (oxygen has not been analyzed). Just beneath the surface a region of the existence of (Fe, Cr)Al phase (according to the binary Fe–Al phase diagram the FeAl phase exists between 30–54 at.% Al at 1075°C) can be recognized. The thickness of this zone which corresponds to the upper layer of the scale is about 100 μm. The strong scatter of the concentration gradients beneath the (Fe, Cr)Al phase (indicated by field 'P' in Fig. 6) results from interactions of the electron beam with pores of the intermediate layer of the scale. A correct quantitative analysis is not possible in this region. For the lower layer of the scale the Al concentration decreases more rapidly than for the upper layer. The Al concentration decreases from 30 to 0 at.% within 120 μm.

The hardness of the upper layer of the scale decreased from about 600 to about 400 HV0.05 with increasing distance from the surface. Beneath the intermediate band of high porosity the hardness of the scale decreased from about 350 to 270 HV0.05 with higher depth. The varying hardness values mirror the change in scale composition across the depth.

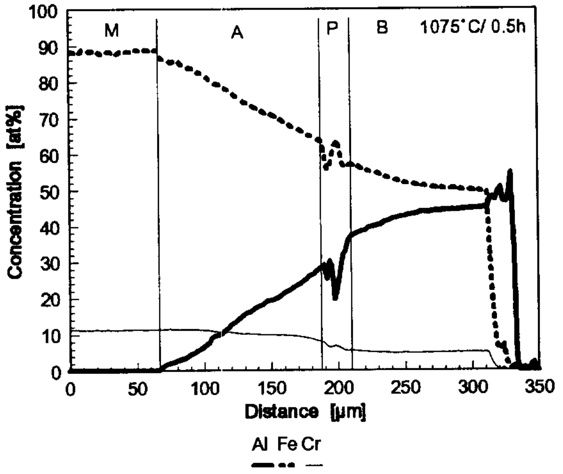

Fig. 6. EPMA line scan of aluminized MANET sample, heat treated at 1075°C for 0.5 h. A: α-Fe(Cr, Al); B: (Fe, Cr)Al; M: matrix; P: band of pores

4. Discussion

The intermetallic scale which has formed during the hot dipping process consists mainly of the (Fe, Cr)$_2$Al$_5$ phase and is very hard and brittle. The brittleness of this phase is demonstrated by several cracks across the scale. The crack propagation direction corresponds to the growth direction of the (Fe, Cr)$_2$Al$_5$ grains. The cracks are probably caused by residual stresses which generated during fast cooling after immersion. Due to the soft matrix material used (MANET II: 250 HV 0.05) the cracks have stopped at the substrate interface. The absence of other Al enriched phases between the (Fe, Cr)$_2$Al$_5$ phase and the substrate, which should exist according to the Fe–Al phase diagram [12], has already been described by several authors [15–17]. This fact indicates a high stability of the (Fe, Cr)$_2$Al$_5$ phase under hot dipping conditions.

The Al overlayer was completely incorporated into the steel after heat treatment at 700°C. Al diffusion along the c-axis of the (Fe, Cr)$_2$Al$_5$ grains is a fast process [18]. The thickness of the (Fe, Cr)$_2$Al$_5$ scale after the incorporation of the Al overlayer is dependent on the thickness of the Al overlayer after the aluminizing process. When the Al reservoir above the sample surface is finished the formation of the (Fe, Cr)$_2$Al$_5$ phase is stopped and the transformation of the (Fe, Cr)$_2$Al$_5$ phase begins at the scale–steel interface. The growth rate of the transformed zone which includes the (Fe, Cr)Al phase and the α-Fe(Cr, Al) solid solution follows a slightly subparabolic growth rate, i.e., during the growth of the transformed zone the diffusion conditions change so that the diffusion processes slow down slightly.

At the (Fe, Cr)$_2$Al$_5$ scale–steel interface the transformation into the (Fe, Cr)Al phase starts. As longer the exposure time as further the reaction front shifts in sample surface direction and the zone of (Fe, Cr)Al phase increases at the expense of the (Fe, Cr)$_2$Al$_5$ scale. A rough estimation of the transformation front between the new formed (Fe, Cr)Al phase and the (Fe, Cr)$_2$Al$_5$ phase by using the equation

$$\Delta x^2 \approx D^* t, \qquad (2)$$

with

$$D^* = c_{\mathrm{Fe}} D_{\mathrm{Al}} + c_{\mathrm{Al}} D_{\mathrm{Fe}} \qquad (3)$$

(x is the thickness of the band of formed (Fe, Cr)Al phase, D^* is the interdiffusion coefficient of Al and Fe, t is the exposure time, $c_{\mathrm{Al,\ Fe}}$ is the concentration of Al and Fe, $D_{\mathrm{Al,\ Fe}}$ is the diffusion coefficients of Al and Fe) leads to an interdiffusion coefficient of Al and Fe of around 7.5×10^{-12} cm^2/s. Assuming a thickness of the (Fe, Cr)$_2$Al$_5$ scale of about 15 μm after incorporation of the excess Al a heat treatment for about 80 h at 700°C is necessary for the complete transformation into the (Fe, Cr)Al phase.

The formed (Fe, Cr)Al phase gets further transformed into the α-Fe(Cr, Al) solid solution at the (Fe, Cr)Al phase–steel interface. The existence of the (Fe, Cr)Al phase between 24 and 50 at.% Al is indicated by the relative shallow slope of the concentration gradient within this range. A kind of plateau has formed comparable to the concentration plateau of the very stable (Fe, Cr)$_2$Al$_5$ phase. These investigations have shown that it is possible to transform the intermetallic (Fe, Cr)$_2$Al$_5$ scale into more ductile phases even at 700°C. However it seems that the exposure time which is necessary for a complete phase transformation is out of a technically relevant range for the investigated aluminized samples since the martensitic steel structure suffers mechanical degradation. For a very thin intermetallic scale of up to about 5 μm a complete phase transformation within an acceptable time range should not be a problem. However, for thicker scales the transformation will remain uncompleted at 700°C and acceptable exposure times.

The investigations have shown that the intermetallic phase could be completely transformed by a heat treatment at 1075°C for 0.5 h. The Al and Fe diffusion is enhanced at higher temperature and therefore the phase transformation at the (Fe, Cr)$_2$Al$_5$–(Fe, Cr)Al and (Fe, Cr)Al–α-Fe(Cr, Al) interfaces proceeds faster than at 700°C. The upper layer of the scale up to the intermediate band of pores consists of (Fe, Cr)Al after the heat treatment. The α-Fe(Cr, Al) phase exists beneath the band of pores. Pores formation at the (Fe, Cr)Al–α-Fe(Cr, Al) interface is probably caused by the different diffusion coefficients of Al and Fe (Kirkendall effect). Al diffuses much faster into the steel than Fe and Cr from the substrate to the (Fe, Cr)Al–α-Fe(Cr, Al) interface. Therefore vacancies are formed at the interface which finally agglomerate to pores. This process was found to be time and temperature dependent since a few pores were observed already after heat treatment at 700°C for 72 h exposure at the (Fe, Cr)Al–α-Fe(Cr, Al) interface. Interesting to note that the α-Fe(Cr, Al) region of the lower layer of the scale shows a similar grain structure as the (Fe, Cr)Al region. This was not the case for samples which were heat treated at 700°C.

5. Summary

The investigations have shown that the transformation of the brittle intermetallic phase (Fe, Cr)$_2$Al$_5$ into the more ductile phases (Fe, Cr)Al and α-Fe(Cr, Al) takes place even at 700°C. A superparabolic growth rate describes this diffusion controlled process which starts at the (Fe, Cr)$_2$Al$_5$-steel substrate interface. At 700°C, only very thin intermetallic scales of about 5 μm can be completely transformed within a technically relevant time period. For thicker intermetallic scales the necessary exposure time would cause mechanical degradation of the martensitic steel. Due to higher diffusion rates at 1075°C the intermetallic scale completely transformed into (Fe, Cr)Al and α-Fe(Cr, Al) even after short exposure times (0.5 h). Pore formation took place at the (Fe, Cr)Al–α-Fe(Cr, Al) interface because of the different diffusion coefficients of Al and Fe in the α-Fe(Cr, Al) zone. Pore formation was found to be a time and temperature dependent process.

Acknowledgements

This work has been performed in the framework of the Nuclear Fusion Project of FZK and was supported by the European Communities within the European Fusion Technology Program.

References

[1] K.S. Forcey, A. Perujo, F. Reiter, P.L. Lolli-Ceroni, J. Nucl. Mater. 200 (1993) 417.
[2] A. Perujo, K.S. Forcey, T. Sample, J. Nucl. Mater. 207 (1993) 86.
[3] L. Giancarli, L. Baraer, M. Eid, M. Fütterer, E. Proust, X. Raepsaet, J.F. Salavy, L. Sedano, Y. Severi, J. Quintric-Bossy, C. Nardi, L. Petrizzi, Fusion Technol. 26 (1994) 1079.
[4] J.D. Fowler, D. Chandra, T.S. Elleman, A.W. Payne, K. Verguese, J. Am. Ceram. Soc. 60 (1977) 155.
[5] H. Glasbrenner, H.U. Borgstedt, J. Nucl. Mater. 212–215 (1994) 1561.
[6] A. Perujo, T. Sample, E. Serra, H. Kolbe, Fusion Technol. 28 (1995) 1256.
[7] G. Benamati, A. Perujo, M. Agostini, A. Serra, N. Antolotti, in: Proc. 18th Symp. on Fusion Technology, Karlsruhe, Germany, 1994 (Elsevier, Amsterdam, 1995) p. 1341.
[8] A. Terlain, E. de Vito, in: Proc. 18th Symp. on Fusion Technology, Karlsruhe, Germany, 1994 (Elsevier, Amsterdam, 1995) p. 1337.
[9] K.S. Forcey, D.K. Ross, C.H. Wu, J. Nucl. Mater. 182 (1991) 36.
[10] G. Benamati, P. Buttol, A. Casagrande, C. Fazio, J. Nucl. Mater. 230 (1996) 214.
[11] H. Glasbrenner, J. Konys, G. Reimann, K. Stein, O. Wedemeyer, in: Proc. 19th Symp. on Fusion Technology, Lisbon, Portugal, 16–20 Sept. 1996, Fusion Technol., to be published.
[12] T.B. Massalski, ed., Binary Alloy Phase Diagrams, 2nd Ed. (ASM International, Metals Park, OH, 1990).
[13] Unpublished X-ray diffraction data.
[14] G. Petzow, G. Effenberg, eds., Ternary Alloys, Vol. 4 (VCH, Weinheim, 1991).
[15] E. Gebhardt, W. Obrowski, Z. Metallkd. 44 (1953) 154.
[16] G. Gürtler, K. Sagel, Z. Metallkd. 46 (1955) 738.
[17] T. Heumann, S. Dittrich, Z. Metallkd. 50 (1959) 617.
[18] G. Eggeler, PhD thesis, Universität Erlangen-Nürnberg (1985).